Phys. Status Solidi C 13, No. 5–6, 248–251 (2016) / DOI 10.1002/pssc.201510180

physica status solidi c
www.pss-c.com
current topics in solid state physics

Room temperature PL efficiency of InGaN/GaN quantum well structures with prelayers as a function of number of quantum wells

George M. Christian*[,1], Simon Hammersley[1], Matthew J. Davies[1], Philip Dawson[1], Menno J. Kappers[2], Fabien C.-P. Massabuau[2], Rachel A. Oliver[2], and Colin J. Humphreys[2]

[1] Photon Science Institute, School of Physics and Astronomy, University of Manchester, Manchester, M13 9PL, UK
[2] Department of Materials Science and Metallurgy, 27 Charles Babbage Road, University of Cambridge, Cambridge, CB3 0FS, UK

Received 29 September 2015, revised 11 December 2015, accepted 15 December 2015
Published online 20 January 2016

Keywords indium gallium nitride, InGaN, quantum wells, prelayer, underlayer

* Corresponding author: e-mail george.christian@manchester.ac.uk, Phone: +44 161 306 4886, Fax: +44 161 275 1031

This is an open access article under the terms of the Creative Commons Attribution Licence, which permits use, distribution and reproduction in any medium, provided the original work is properly cited.

We report on the effects of varying the number of quantum wells (QWs) in an InGaN/GaN multiple QW (MQW) structure containing a 23 nm thick $In_{0.05}Ga_{0.95}N$ prelayer doped with Si. The calculated conduction and valence bands for the structures show an increasing total electric field across the QWs with increasing number of QWs. This is due to the reduced strength of the surface polarisation field, which opposes the built-in field across the QWs, as its range is increased over thicker samples. Low temperature photoluminescence (PL) measurements show a red shifted QW emission peak energy, which is attributed to the enhanced quantum confined Stark effect with increasing total field strength across the QWs. Low temperature PL time decay measurements and room temperature internal quantum efficiency (IQE) measurements show decreasing radiative recombination rates and decreasing IQE, respectively, with increasing number of QWs. These are attributed to the increased spatial separation of the electron and hole wavefunctions, consistent with the calculated band profiles. It is also shown that, for samples with fewer QWs, the reduction of the total field across the QWs makes the radiative recombination rate sufficiently fast that it is competitive with the efficiency losses associated with the thermal escape of carriers.

1 Introduction InGaN/GaN quantum wells (QWs) are regularly incorporated in the active regions of high-efficiency blue light emitting diodes (LEDs). External quantum efficiencies as high as 70% [1] occur in *c*-plane wurtzite (In)GaN despite the large built-in electric field across the QWs due to the discontinuities in the spontaneous polarisation at the interfaces between GaN and InGaN layers, and the piezoelectric polarisation due to the strain in the InGaN layers grown on GaN [2]. There have been several reports [3–13] that the growth of a layer of InGaN, 10s of nm thick and referred to as a prelayer, prior to the first QW in multiple QW (MQW) structures and LEDs leads to increases in the measured luminescence intensity and room temperature (RT) internal quantum efficiency (IQE). Suggestions for the mechanism by which prelayers bring about these improvements have included strain reduction in the QW layers [3], acting as an “electron reservoir” from which carriers tunnel into the QWs [4], and a reduction in the density of point defects in the active region [5,8–10]. We have previously demonstrated [11–13] that the QW IQE improvements associated with the inclusion of prelayers can be explained as being due to the modification of the surface polarisation field between the sample surface and the prelayer which opposes the fields across the QWs. This leads to a reduction in the net electric fields across all of the QWs in the stack. Increased

© 2016 The Authors. *Phys. Status Solidi C* published by WILEY-VCH Verlag GmbH & Co. KGaA, Weinheim

RT IQEs and 10 K radiative recombination rates were observed in structures containing 1 and 10 $In_{0.16}Ga_{0.84}N$/GaN QWs with prelayers compared with structures that did not contain prelayers. In this paper we report on the effects of varying the number of QWs in InGaN/GaN MQW structures, all containing a Si doped InGaN prelayer, on the calculated band profiles and measured optical properties.

2 Experimental details The structures studied consisted of 1, 3, 5, 7, 10 and 15 $In_{0.12}Ga_{0.88}N$/GaN QWs, labelled as samples 1QW-15QW respectively. The structures were grown by MOVPE on top of 5 μm thick GaN pseudo-substrates with a threading dislocation density of $\sim 4 \times 10^8$ cm^{-2} grown on *c*-plane sapphire substrates. For all of the samples, a 2 μm GaN template doped with Si to a nominal density of 5×10^{18} cm^{-3} was grown followed by a 23 nm $In_{0.05}Ga_{0.95}N$ prelayer with the same nominal Si doping density. On top of the prelayer was then grown a 3 nm layer of unintentionally ($< 10^{17}$ cm^{-3}) doped GaN followed by the InGaN QW(s) and GaN barrier(s). The QWs and barriers had nominal thicknesses of 2.3 nm and 7 nm, respectively, and were grown using the two-temperature (2T) growth method [14]. X-ray diffraction (XRD) measurements performed on each sample found all of the QWs and barriers in all of the structures to have thicknesses of 2.3 ± 0.1 nm and 7.0 ± 0.1 nm, respectively. The presence of gross well width fluctuations, a result of the 2T growth method, means that XRD cannot uniquely characterise the thickness and composition of the QWs. Nevertheless an equivalent uniform QW thickness and composition can be obtained. The In compositions of the QWs were indistinguishable in samples 3QW-15QW with a value of 12 ± 1 %. For sample 1QW the In content was determined to be lower at 8 ± 1 %, assuming a constant well width of 2.3 nm.

The optical properties of the structures were studied by measuring the photoluminescence (PL) spectra as a function of temperature, and the PL decay transients at 10 K. The samples were mounted on the cold finger of a temperature controlled closed-cycle helium cryostat and inclined at Brewster's angle with respect to the collection axis to minimise the effects of Fabry-Pérot interference oscillations on the PL spectra [15]. For the temperature dependent PL measurements, a CW He/Cd laser with a photon energy of 3.815 eV was used as the excitation source. For the PL decay time measurements, a frequency tripled mode-locked Ti:sapphire laser system with a final photon energy of 4.881 eV was used as the excitation source and the PL decay transients were measured using a time-correlated single photon counting system.

3 Results and discussion The conduction and valence band profiles of the structures were calculated using the commercially available device simulation package nextnano^3 [16] using their experimentally determined structural and compositional parameters. The calculated

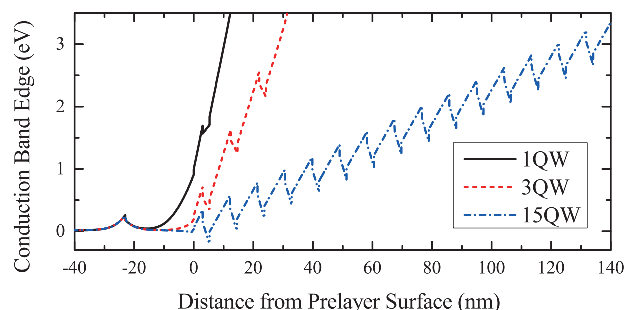

Figure 1 Calculated conduction band profiles for samples 1QW, 3QW and 15QW.

conduction band profiles for samples 1QW, 3QW and 15QW are shown in Fig. 1. For all of the samples, the Fermi energy is pinned just below the conduction band edge by the *n*-type doping in the region of the prelayer and at the valence band edge by the surface charges formed at the GaN/air interface at the sample surface [2]. This leads to significant tilting of the conduction and valence bands resulting in a surface polarisation field, which opposes the built-in polarisation fields across the QWs. With decreasing distance between the prelayer and the sample surface, the strength of the surface polarisation field increases and so the strengths of the total fields across the QWs are reduced (Fig. 2). Notably, the surface field acting across sample 1QW is sufficiently strong that the sign of the total field across the QW is reversed relative to an InGaN/GaN QW without a prelayer (for example reference [17]).

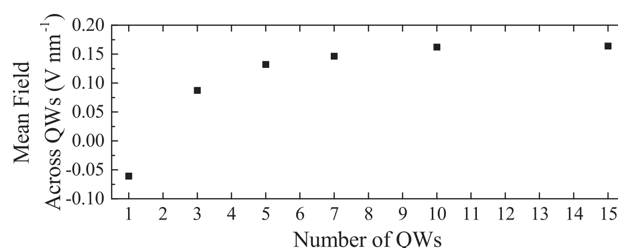

Figure 2 Mean fields across QWs for each sample as a function of the number of QWs.

PL emission spectra obtained at low temperature ($T =$ 10 K), using an excitation power density of 15 W cm^{-2}, are shown for samples 1QW, 3QW and 15QW in Fig. 3. The PL emission from the QWs lies between 2.7 and 2.8 eV for all of the samples. An additional emission feature at 3.28 eV is attributed to recombination in the prelayer. In general and allowing for variation within the sample, the peak energy of the QW emission feature red shifts with increasing number of QWs (Fig. 4). This is attributed to the increasing total field across a QW, leading to an enhanced quantum confined Stark effect (QCSE) [18], consistent

 © 2016 The Authors. *Phys. Status Solidi C* published by WILEY-VCH Verlag GmbH & Co. KGaA, Weinheim

with the calculated band profiles. It should be noted that the lower In content determined for sample 1QW would also contribute to its higher QW PL emission energy. However, we calculate that the prelayer provides the dominant contribution.

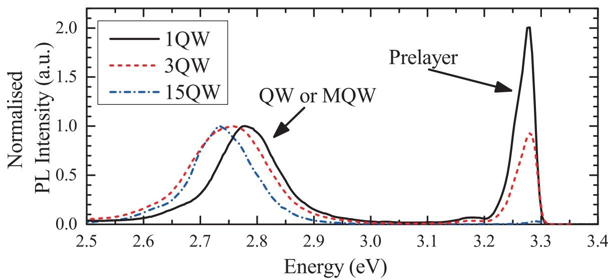

Figure 3 PL spectra at $T = 10$ K for samples 1QW, 3QW and 15QW. Emission features corresponding to the QWs and the prelayer are highlighted. Intensities have been normalised to the peak QW emission intensity for each sample.

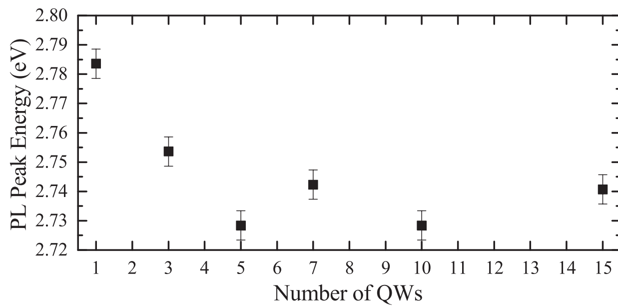

Figure 4 Peak PL emission energy at $T = 10$ K varying with number of QWs.

PL decay transients were obtained at $T = 10$ K, at which temperature the decay is assumed to be solely radiative, at the QW peak energy for each sample using an excitation energy density per pulse of 9.90 µJ cm^{-2} and are shown for samples 1QW, 3QW, and 15QW in Fig. 5. The non-exponential shape of the decay transients, attributed to the variation in the in-plane separation of the independently localised electrons and holes [19], means that they cannot be described using a single decay constant. Instead, we characterise the PL decay time scale by the time required for the PL intensity to fall to 1/e of its maximum value ($\tau_{1/e}$). The measured value of $\tau_{1/e}$ is 5.0 ns for sample 1QW and increases with increasing number of QWs up to 16.6 ns for sample 15QW. In Fig. 6, the value of $\tau_{1/e}$ is shown to increase with increasing magnitude of the mean field across the QWs. The change in $\tau_{1/e}$ reflects qualitatively the change in the total electric fields across the QWs predicted by the calculated band profiles, and faster radiative recombination rates are attributed to weaker total electric fields across the QWs in a sample due to the reduced spatial separation of the electron and hole wavefunctions [20].

One source of efficiency loss in InGaN/GaN QW structures and LEDs is the thermal escape of carriers from the QW confining potential before they recombine [21,22]. The RT IQE of InGaN/GaN MQW structures, and LEDs, without prelayers has been measured to increase with increasing number of QWs, an effect which has been attributed to the recapture of carriers by adjacent QWs [23, 24]. To investigate the effects of the band profile modifications by the prelayer on this process, the temperature dependences of the PL from the structures in our study were obtained using the same excitation conditions as the low temperature PL spectra described above. Between $T = 10$ K and $T = 80$ K, the prelayer emission feature was found to quench rapidly with increasing temperature while the PL intensity from the (M)QW increased over this range, before decreasing as T was increased from 80 K to 300 K. This effect was most dramatic for the samples with fewest QWs. The RT IQE was therefore defined as the ratio of the integrated PL intensity at RT to that at 80 K. This was found to decrease with increasing number of QWs (Fig. 7). This indicates that the increase in the radiative recombination rate is sufficient to compete with the efficiency lost due to the thermal escape of carriers.

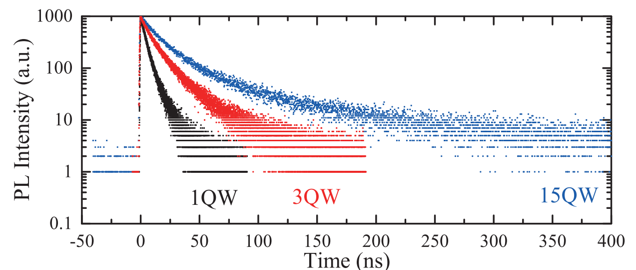

Figure 5 PL decay transients at $T = 10$ K for samples 1QW, 3QW and 15QW.

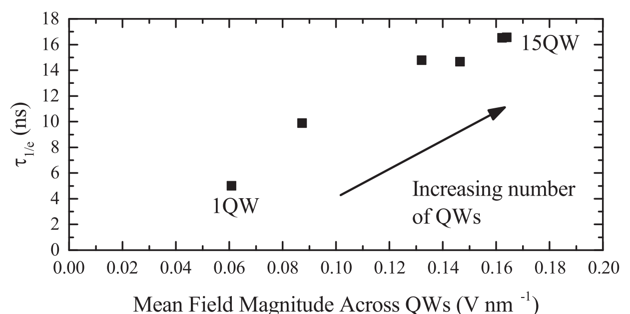

Figure 6 1/e PL decay lifetimes ($\tau_{1/e}$) at $T = 10$ K varying with the mean field across the QWs. The points corresponding to samples 1QW and 15QW are labelled, and the number of QWs in a sample increases with the calculated mean field. Note that it is the magnitude of the mean field that is shown here.

© 2016 The Authors. *Phys. Status Solidi C* published by WILEY-VCH Verlag GmbH & Co. KGaA, Weinheim

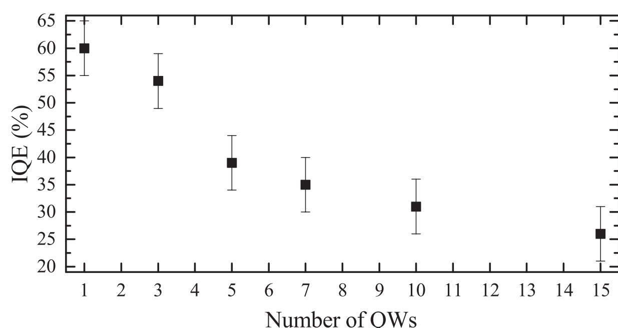

Figure 7 RT IQE defined relative to that at 80 K varying with number of QWs.

4 Summary In summary, six $In_{0.12}Ga_{0.84}N$ MQW structures with varying numbers of QWs containing Si doped $In_{0.05}Ga_{0.95}N$ prelayers were grown and their conduction and valence band profiles were calculated. The calculated total electric field across the QWs in each structure was found to increase with increasing number of QWs, due to the reduced strength of the surface polarisation field with increasing separation between the prelayer and the GaN/air interface. We measured a red shift in the (M)QW PL emission energy and a decrease in the radiative recombination rate with increasing number of QWs. Both are evidence of a reduced field across the QWs in the structures with fewer QWs compared with those with more QWs, consistent with the calculated trend in the strength of the total field across the QWs. The variation in the radiative recombination rate between the structures also indicates a modification of the competition between radiative, nonradiative and carrier escape processes. A consequence of this is the observed RT IQE decrease with increasing number of QWs. This is the opposite behaviour to that previously observed in InGaN/GaN MQW structures that do not contain prelayers. For those structures, the increase in the RT IQE with increasing number of QWs is attributed to the recapture of carriers by the additional QWs. The inclusion of a prelayer therefore leads to an improved radiative rate that is sufficiently rapid to compete with the loss in IQE due to thermal escape of carriers when the number of QWs is reduced.

Acknowledgements This work was carried out with the support of the United Kingdom Engineering and Physical Sciences Research Council under Grant Nos. EP/I012591/1 and EP/H011676/1.

References

[1] M. J. Cich, R. I. Aldaz, A. Chakraborty, A. David, M. J. Grundmann, A. Tyagi, M. Zhang, F. M. Steranka, and M. R. Krames, Appl. Phys. Lett. **101**(22), 1–4 (2012).

[2] O. Mayrock, H. J. Wünsche, and F. Henneberger, Phys. Rev. B **62**(24), 870–880 (2000).

[3] N. Nanhui, W. Huaibing, L. Jianping, L. Naixin, X. Yanhui, H. Jun, D. Jun, and S. Guangdi, Solid. State Electron. **51**(6), 860–864 (2007).

[4] N. Otsuji, K. Fujiwara, and J. K. Sheu, J. Appl. Phys. **100**(11), 113105 (2006).

[5] A. M. Armstrong, B. N. Bryant, M. H. Crawford, D. D. Koleske, S. R. Lee, and J. J. Wierer, J. Appl. Phys. **117**(13), 134501 (2015).

[6] T. Akasaka, H. Gotoh, T. Saito, and T. Makimoto, Appl. Phys. Lett. **85**(15), 3089–3091 (2004).

[7] T. Akasaka, H. Gotoh, H. Nakano, and T. Makimoto, Appl. Phys. Lett. **86**(19), 191902 (2005).

[8] T. Akasaka, H. Gotoh, Y. Kobayashi, H. Nakano, and T. Makimoto, Appl. Phys. Lett. **89**(10), 101110 (2006).

[9] P. T. Törmä, O. Svensk, M. Ali, S. Suihkonen, M. Sopanen, M. A. Odnoblyudov, and V. E. Bougrov, J. Cryst. Growth **310**(23), 5162–5165 (2008).

[10] J. K. Son, S. N. Lee, T. Sakong, H. S. Paek, O. Nam, Y. Park, J. S. Hwang, J. Y. Kim, and Y. H. Cho, J. Cryst. Growth **287**, 558–561 (2006).

[11] M. J. Davies, F. C. P. Massabuau, P. Dawson, R. A. Oliver, M. J. Kappers, and C. J. Humphreys, Phys. Status Solidi C **11**(3-4), 710–713 (2014).

[12] M. J. Davies, P. Dawson, F. C. P. Massabuau, R. A. Oliver, M. J. Kappers, and C. J. Humphreys, Appl. Phys. Lett. **105**(9), 092106 (2014).

[13] M. J. Davies, P. Dawson, F. C. P. Massabuau, A. L. Fol, R. A. Oliver, M. J. Kappers, and C. J. Humphreys, Phys. Status Solidi B **252**(5), 866–872 (2015).

[14] R. A. Oliver, F. C. P. Massabuau, M. J. Kappers, W. A. Phillips, E. J. Thrush, C. C. Tartan, W. E. Blenkhorn, T. J. Badcock, P. Dawson, M. A. Hopkins, D. W. E. Allsopp, and C. J. Humphreys, Appl. Phys. Lett. **103**(14), 141114 (2013).

[15] D. M. Graham, A. Soltani-Vala, P. Dawson, M. J. Godfrey, T. M. Smeeton, J. S. Barnard, M. J. Kappers, C. J. Humphreys, and E. J. Thrush, J. Appl. Phys. **97**(10), 103508 (2005).

[16] S. Birner, nextnano GmbH.

[17] D. A. Browne, B. Mazumder, Y. R. Wu, and J. S. Speck, J. Appl. Phys. **117**(18), 185703 (2015).

[18] T. Takeuchi, S. Sota, M. Katsuragawa, M. Komori, H. Takeuchi, H. Amano, and I. Akasaki, Jpn. J. Appl. Phys. **36**(Part 2, No. 4A), L382–L385 (1997).

[19] A. Morel, P. Lefebvre, S. Kalliakos, T. Taliercio, T. Bretagnon, and B. Gil, Phys. Rev. B **68**(4), 045331 (2003).

[20] J. Seo Im, H. Kollmer, J. Off, A. Sohmer, F. Scholz, and A. Hangleiter, Phys. Rev. B **57**(16), R9435–R9438 (1998).

[21] I. A. Pope, P. M. Smowton, P. Blood, J. D. Thomson, M. J. Kappers, and C. J. Humphreys, Appl. Phys. Lett. **82**(17), 2755–2757 (2003).

[22] M. H. Kim, M. F. Schubert, Q. Dai, J. K. Kim, E. F. Schubert, J. Piprek, and Y. Park, Appl. Phys. Lett. **91**(18), 183507 (2007).

[23] P. Hurst, P. Dawson, S. Levetas, M. Godfrey, I. Watson, and G. Duggan, Phys. Status Solidi B **228**(1), 137–140 (2001).

[24] A. Laubsch, M. Sabathil, J. Baur, M. Peter, and B. Hahn, IEEE Trans. Electron Devices **57**(1), 79–87 (2010).

© 2016 The Authors. *Phys. Status Solidi C* published by WILEY-VCH Verlag GmbH & Co. KGaA, Weinheim